ISSN 1027-5495. Functional Materials, 25, No.1 (2018), p. 28-33.
doi:https://doi.org/10.15407/fm25.01.28

$CaWO_4$@$MPSiO_2$ nanocomposite: synthesis and characterization

***K.Hubenko*[1], *I.Bespalova*[1], *P.Maksimchuk*[1], *P.Mateychenko*[2], *R.Grynyov*[3], *S.Yefimova*[1]**

[1]Institute for Scintillation Materials, STC "Institute for Single Crystals", National Academy of Sciences of Ukraine, 60 Nauky Ave., 61072 Kharkiv, Ukraine
[2]Institute for Single Crystals, STC "Institute for Single Crystals", National Academy of Sciences of Ukraine, 60 Nauky Ave., 61072 Kharkiv, Ukraine
[3]Ariel University, Natural Science Faculty, Physics Department, P.O.B. 3, 407000 Ariel, Israel

Received October 24, 2017

The features of obtaining a nanocomposite consisting of the $CaWO_4$ core which is a scintillation nanocrystal and a mesoporous SiO_2 shell ($CaWO_4$@$MPSiO_2$) are considered. The results of the investigation of microscopic and optical parameters of $CaWO_4$@$MPSiO_2$ nanocomposite are presented. The mesoporous SiO_2 shell applied to the nanocrystal can be used both as a host for the photosensitizer, and set the necessary distance between the donor and the energy acceptor.

Keywords: Nanocomposite, $CaWO_4$, Mesoporous SiO_2, X-Ray Induced Photodynamic Therapy.

Рассмотрены особенности получения нанокомпозита, состоящего из ядра $CaWO_4$, представляющего собой сцинтилляционный нанокристал, и мезопористой SiO_2 оболочки ($CaWO_4$@$MPSiO_2$). Представлены результаты исследования микроскопических и оптических параметров нанокомпозита $CaWO_4$@$MPSiO_2$. Нанесенная на нанокристалл мезопористая SiO_2 оболочка может использоваться как в качестве хоста для фотосенсибилизатора, так и задавать необходимое расстояние между донором и акцептором энергии.

$CaWO_4$@$MPSiO_2$: синтез та характеристика. *К.Губенко, І.Беспалова, П.Максимчук, П.Матейченко, Р.Гриньов, С.Єфімова.*

Розглянуто особливості отримання нанокомпозиту, що складається з ядра $CaWO_4$, який представляє собою сцинтиляційний нанокристал та мезопористої SiO_2 оболочки. Приведено результати досліджень мікроскопічних і оптичних параметрів нанокомпозиту $CaWO_4$ у мезопористій SiO_2 оболочці. Нанесена на нанокристал мезопориста оболочка може використовуватися як в якості хоста для фотосенсибілізатора, так і задавати необхідну відстань між донором і акцептором енергії.

1. Introduction

Photodynamic therapy (PDT) — method of local activation of the photosensitizer (PS) accumulated in the tumor by visible red light, which in the presence of tissue oxygen leads to the production of free radicals and reactive oxygen species (ROS) including singlet oxygen ($^1O_2$) due to electron or energy transfer from excited PS to oxy-

gen molecules and substrate [1, 2]. It is commonly accepted that singlet oxygen is the predominant cytotoxic agent produced during PDT [3, 4].

For deep cancer treatment, the light should be within the near infrared NIR range of 700–1100 nm, where most tissue chromophores, including oxyhemoglobin, deoxyhemoglobin, melanin, and fat, weakly absorb [5]. Unfortunately, most available PS has absorption bands at wavelengths shorter than 700 nm. Recently, to solve this problem and enhance the PDT treatment for deep cancers, a new concept has been proposed by Chen and co-authors [6]. This modern approach is based on the use of scintillation nanoparticles (ScNPs) as energy transducers, which transform X-ray to UV/visible photons, and act as an energy source for PS molecules to activate PDT [7–12]. One of the main advantages of X-ray-induced photodynamic therapy (X-PDT), unlike traditional PDT, is the absence of restrictions on the depth of the excitation light penetration into biological tissues [13]. A typical mechanism for energy transfer between ScNPs and PS is non-radiative (Forster) resonance energy transfer (FRET). In such systems scintillation NPs act as an excitation energy donor, whereas PS molecules as energy acceptors [14, 15]. To create efficient ScNPs — PS complexes, potential donor — acceptor pairs should meet one of the main requirement, mainly, overlapping the acceptor absorption spectrum with the donor luminescence one [16].

One of the most effective PS is Protoporphyrin IX [17]. The maximum of its absorption spectrum is in the range of 400–410 nm. Therefore, in order to ensure efficient energy transfer in the complex "ScNPs–PS", the nanoparticle should be characterized by intense X-ray luminescence in the same range. As one of the suitable candidates, one can consider nanoparticles of tungstates, in particular calcium tungstate ($CaWO_4$). This is due to the good biological compatibility of this material [18], intensive luminescence of $CaWO_4$ [19], and overlapping of its luminescence spectrum with the absorption spectrum of PS, as Protoporphyrin IX [17].

The second basic requirements for the realization of non-radiative excitation energy transfer from the ScNPs to the PS molecules is the distance between the energy donor (ScNPs) and the energy acceptor (PS molecules), which is governed by the FRET pair spectral overlap and is usually in the range of 1–10 nm [16]. There are currently various strategies for ScNPs binding with PS molecules, including physical PS loading, covalent conjugation, direct ScNPs surface coating and mesoporous silica coating loaded with PS [20].

In this paper, we report the synthesize and characterization of $CaWO_4$@$MPSiO_2$ nanocomposite, consisting of a $CaWO_4$ ScNPs core and a mesoporous SiO_2 shell, which can be used both as a host for the PS molecules and to set the required distance between ScNPs core and loaded PS.

2. Experimental

2.1. Materials

Calcium chloride ($CaCl_2$, Khimlabreaktiv, Ukraine), ammonia water 25 mas. % (NH_4OH, Khimlabreaktiv, Ukraine), citrate sodium crystalline hydrate ($Na_3Cit*5H_2O$, Khimlabreaktiv, Ukraine) were analytical reagents and used as received.

Tetraethyl orthosilicate ($Si(OC_2H_5)_4$, TEOS, 98 %), cetyltrimethylammonium bromide ($CH_3(CH_2)_{15}N(Br)(CH_3)_3$, CTAB, 95 %), sodium tungstate hydrate ($Na_2WO_4 \cdot 2H_2O$, 99 %) were purchased from Sigma-Aldrich (USA) and used as received.

2.2. Instrumentation and characterization

Synthesized $CaWO_4$@$MPSiO_2$ nanocomposite was characterized by scanning electron microscopy (SEM, JSM-6390LV, (JEOL Company, USA), operated at 15 kV and Ultra-High Resolution Scanning Electron Microscopy (MAIA3 TESCAN, Czech Republic, EU), operated at 15 kV) and transmission electron microscopy (TEM, JEM-2100F (JEOL Company, Japan)) operated at 200 kV, equipped with an Oxford CCD camera.

The X-ray diffraction pattern was measured with a PANalytical X'Pert Pro X-RAY diffractometer. The data were analyzed using the Program X'Pert HighScore Plus (Version 2.2e), which allowed comparisons with the ICCD X-ray diffraction pattern database (PDF Release-2, 2009).

Zeta-potential of the $CaWO_4$@$MPSiO_2$ nanocomposite was measured with a Zeta-PALS analyzer (Brookhaven Instruments Corp., USA) operated in a phase analysis light scattering mode.

The photoluminescence and excitation spectra were recorded by means of automatic spectrofluorimeter based on the lattice monochromator MDR-23. The photomulti-

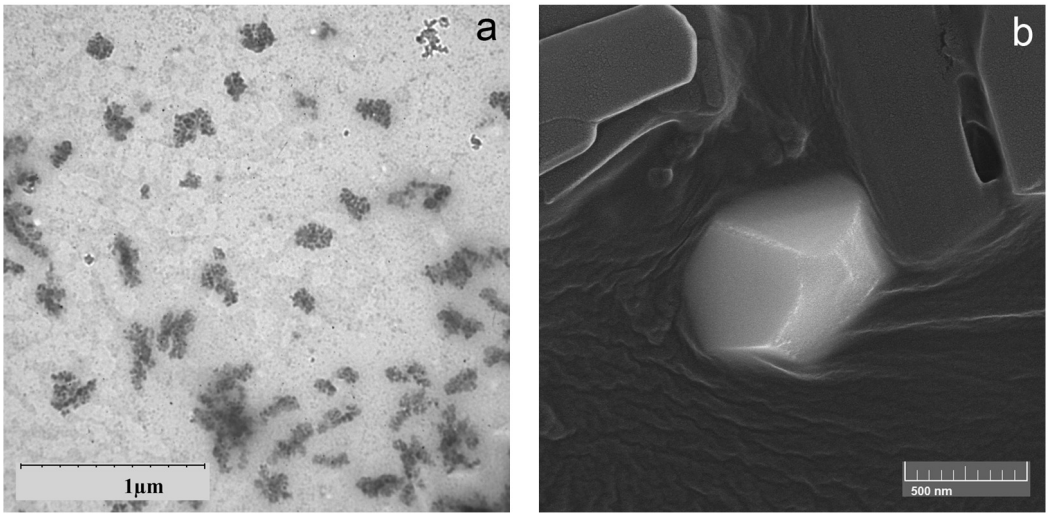

Fig. 1. TEM images of the amorphous agglomerates $CaWO_4$ (a) and SEM images of the $CaWO_4$ nanocrystal (b).

plier Hamamatsu R9110 operating in the photon counting mode had been used for luminescence spectra registration. The Xenon-lamp coupled with monochromator MDR-206 had been used as the photoluminescence excitation source.

The X-ray luminescence has been excited by an X-ray generator "REYS" (U = 25 kV, I = 37 μA), and registered using the MDR-23 grating monochromator with the Hamamatsu R9110 PMT in the photon counting mode.

All measurements were carried out at room temperature.

3. Results and discussion

3.1. Synthesis and characteristics of $CaWO_4$ nanoparticles

$CaWO_4$ amorphous nanoparticles were obtained by the colloidal method [21]. First, 10 mL of sodium citrate (C (Na_3Cit) = 0.225 M) was mixed with 10 mL of calcium chloride solution (C ($CaCl_2$) = 0.300 M). Then 10 mL of sodium tungstate (C ($NaWO_4$) = 0.45 M) was poured into the mixture under vigorous stirring. The resulting mixture was heated with constant stirring in a water bath to 65°C. The resulting slurry of amorphous calcium tungstate $CaWO_4$ was placed in a dialysis bag (molecular weight of 12,000 Da and 2.5 nm pore diameter) and the dialysis was conducted at room temperature for 5 h, changing the distilled water every hour to a value pH ~ 7,0. Then the suspension was evaporated on a water bath for powdered amorphous calcium tungstate $CaWO_4$. Obtained TEM images show $CaWO_4$ amorphous agglomerates of about 300 nm size (Fig. 1a), which are composed on $CaWO_4$ nanoparticles of about 10–20 nm size. These particles do not possess luminescence. To obtain required crystal structure and subsequently luminescent properties, amorphous $CaWO_4$ particles were coated with thin SiO_2 solid shell and annealed at high temperature.

For this purpose, 0.05 g amorphous $CaWO_4$ were treated with 20 mL ethanol under ultrasonication for 30 min. Then the particles were well dispersed in a mixture of 20 mL ethanol, deionized 10 mL water, and 0.5 mL concentrated ammonia solution. Then 0.03 mL TEOS was added dropwise to the solution. After being stirred for 4 h at room temperature, the products were separated, dried at 50°C overnight and annealing at 900°C for 2 h. As a result, the $CaWO_4$ nanocrystals were obtained (see. Fig. 1b).

XRD analysis was used to study the crystal structures of the $CaWO_4$ nanoparticles. XRD pattern of the $CaWO_4$ nanocrystals exhibits the characteristic reflections of scheelite (Fig. 2).

3.2. Synthesis and characteristics of $CaWO_4$@$MPSiO_2$ nanocomposite

To cover the obtained $CaWO_4$ nanocrystals with mesoporous silica layer, we use the procedure described in [22], where spheres with the Fe_3O_4 core with surface area 676 $m^2 \cdot g^{-1}$ and total pore volume 0.46 $cm^3 \cdot g^{-1}$ at a nanocomposite particle size of 500 nm were obtained.

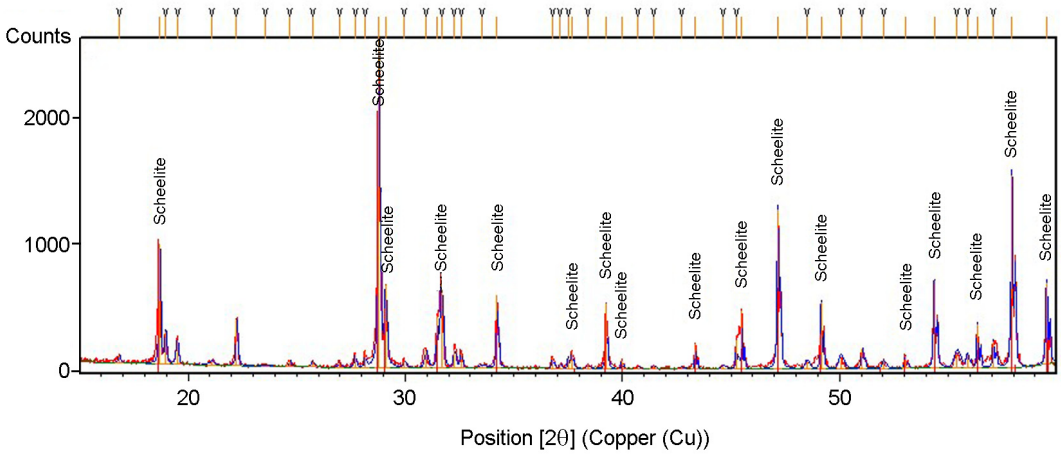

Fig. 2. XRD analysis of $CaWO_4$ nanocrystals.

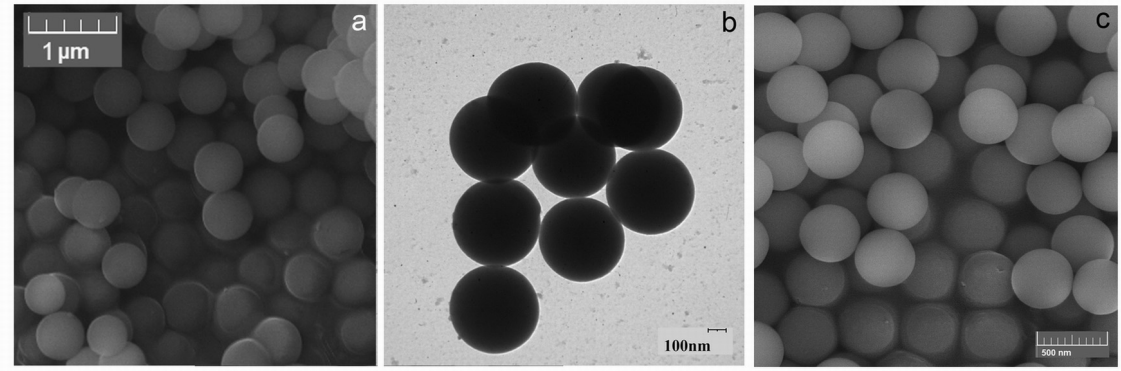

Fig. 3. SEM (a) and TEM (b) images of the $CaWO_4$@$MPSiO_2$ nanocomposite and SEM images of the blank SiO_2 (c).

For deposition of the mesoporous SiO_2 shell 0.02 g of $CaWO_4$@solid SiO_2 were redispersed in a mixed solution containing of 0.075 g CTAB, 20 mL deionized water, 0.30 mL concentrated ammonia solution and 15 mL ethanol. The resulting solution was stirred for 30 min. Then, 0.20 mL TEOS was added dropwise to the solution with vigorous stirring. After reaction for 4 h, the product was centrifuged, washed repeated with ethanol and distilled water.

Finally, the CTAB templating agents were removed using an acid extraction process: the synthesized $CaWO_4$@$MPSiO_2$ nanocomposite (residual sediment) were suspended in a solution of 25 mL ethanol and 1.25 mL HCl with a concentration 2 M. The suspension was vigorously stirred for 48 h, and the products were centrifuged, washed with ethanol and distilled water in sequence, and dried at 50°C for 2 h.

As a result, the obtained $CaWO_4$@$MPSiO_2$ nanocomposite of spherical shape with the average sphere diameter d ~ 500 nm and with a minimum spread in size is presented in Fig. 3a, b. Zeta-potential of the synthesized $CaWO_4$@$MPSiO_2$ nanocomposite is +8.12±0,01 mV. The slight positive charge of the obtained nanospheres is governed by the residual of positively charged surfactant CTAB molecules using as a templating agent.

Also, we have prepared blank sample SiO_2 by the same procedure only without a scintillation core for comparison with $CaWO_4$@$MPSiO_2$ nanocomposite. Obtained SEM images show SiO_2 sphere (Fig. 3c).

XRD analysis showed that the obtained $CaWO_4$@$MPSiO_2$ nanocomposite consists of the $CaWO_4$ core, the solid SiO_2 shell, and the mesoporous SiO_2 shell. Roentgenogram showed reflexes from all phases (Fig. 4).

3.3 Optical properties of the $CaWO_4$@$MPSiO_2$ nanocomposite

Figure 5a shows the excitation and luminescence spectra of the obtained $CaWO_4$@$MPSiO_2$ nanocomposite. The excitation spectrum of the synthesized nanocomposite (Fig. 5a, curve *1*) consists of the sin-

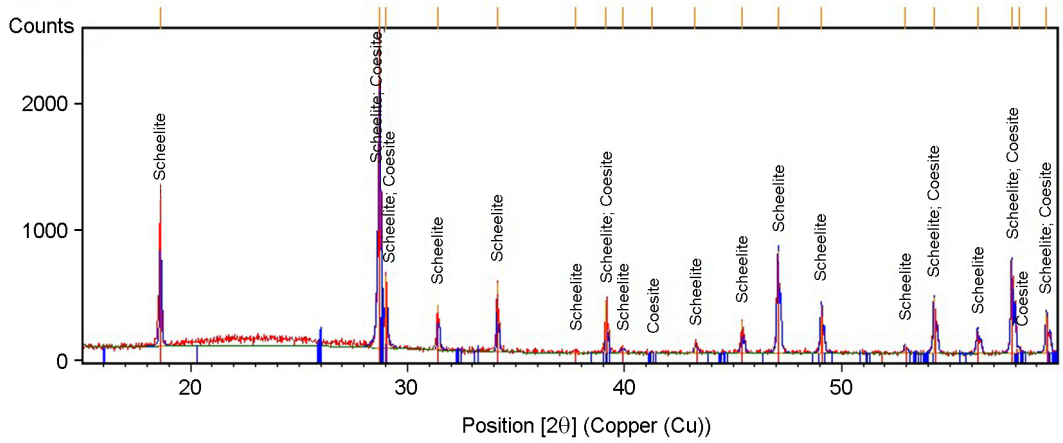

Fig. 4. XRD analysis of the $CaWO_4$@$MPSiO_2$ nanocomposite.

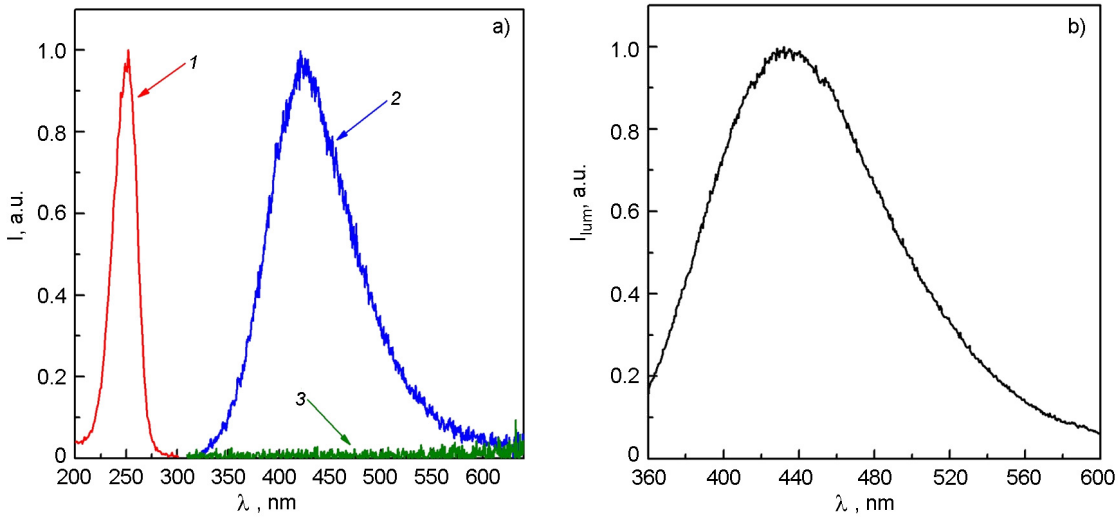

Fig. 5. Photoluminescence properties of obtained samples (a): curve *1* — excitation spectrum for emission λ_{exc} = 440 nm of the $CaWO_4$@$MPSiO_2$ nanocomposite, curve *2* — emission spectrum of the $CaWO_4$@$MPSiO_2$ nanocomposite under excitation λ_{exc} = 260 nm, curve *3* — emission spectrum of blank SiO_2 under excitation λ_{exc} = 260 nm; emission spectrum of the $CaWO_4$@$MPSiO_2$ nanocomposite under X-ray excitation (b), T = 293 K.

gle band centered at about 250 nm. This band corresponds to electron transfer from 2*p* oxygen orbitals to the 5*d* tungsten orbitals.

The luminescence spectrum consists of the broad emission band centered at about 435 nm (Fig. 5a, curve *2*), which is due to electronic transitions of the charge-transfer type between tungstate and oxygen within the anion complex WO_4^{2-} in $CaWO_4$ [23, 24]. The shape of the band and the position of its maximum coincide with the luminescence band of a bulk crystal [25].

In should be noted that the blank SiO_2 do not possess luminescence in the spectral range (Fig. 5a, curve *3*).

For X-PDT applications, it is necessary that the core of the nanocomposite be characterized by intense X-ray induced luminescence. The luminescence spectrum of the investigated $CaWO_4$@$MPSiO_2$ nanocomposite under X-ray excitation at room temperature is a broad band with a maximum at 435 nm (Fig. 5b). This band is associated with the $CaWO_4$ host lattice. It is corresponds with radiative relaxation of excitation of anion complex WO_4^{2-} with electron transfer from 5*d* W to 2*p* O [26].

4. Conclusions

$CaWO_4$@$MPSiO_2$ nanocomposite with size d = 500 nm were synthesized and characterized by various techniques.

XRD analysis showed that the obtained $CaWO_4$@SiO_2 nanocomposite consists of the $CaWO_4$ core, the solid SiO_2 shell, and the mesoporous SiO_2 shell. Roentgenogram showed reflexes from all phases.

The photo- and X-ray-luminescence spectra of the resulting nanocomposite with maximum $\lambda = 435$ nm correspond to the luminescence of crystalline calcium tungstate.

Obtained nanocomposite can realize the necessary conditions for energy transfer from the X-ray-induced nanoparticle to the PS. The experimental results indicate high potential of the $CaWO_4$@$MPSiO_2$ nanocomposite as carriers for encapsulation of organic dye molecules, for instance, PS PPIX, used in PDT.

References

1. D.Dolmans, D.Fukumura, R.Jain, *Nat. Rev. Cancer*, **3**, 380 (2003).
2. S.Yano, S.Hirohara, M.Obata et al., *J. Photochem. Photobiol. C: Photochem. Rev.*, **1**, 46 (2011).
3. C.N.Zhou, *J. Photochem. Photobiol., B*, **3**, 299 (1989).
4. R.Allison, G.Downie, R.Cuenca et al., *Photodiag. and Photodynam. Therapy*, **1**, 27 (2004).
5. V.Ntziachristos, C.Bremer, R.Weissleder, *Europ. J. Radiology*, **13**, 195 (2003).
6. W.Chen, J.Zhang, *J. Nanosci. Nanotechnol.*, **6**, 1159 (2006).
7. K.Kirakci, P.Kubat, K.Fejfarova, *Inorg. Chem.*, **2**, 803 (2016).
8. S.Lucky, K.Soo, Y.Zhang, *Chem. Rev.*, **115**, 1990 (2015).
9. W.Chen, J.Zhang, *J. Nanosci. Nanotechnol.*, **6**, 1159 (2006).
10. A.-L.Bulin, C.Truillet, R.Chouikrat et al., *J. Phys. Chem. C*, **117**, 21583 (2013).
11. Y.Tang, J.Hu, A.Elmenoufy et al., *ACS Appl. Mater. & Interfaces*, **7**, 12261 (2015).
12. H.Chen, G.Wang, Y.-J.Chuang et al., *J. Nano Lett.*, **15**, 2249 (2015).
13. P.Retif, S.Pinel, M.Toussaint et al., *Theranostics*, **5**, 1030 (2015).
14. S.Lindhoud, A.Westphal, C.P.M.van Mierlo et al., *Int. J. Molecul. Scie.*, **15**, 23836 (2014).
15. J.Lee, M.Brennan, R.Wilton et al., *Nano Lett.*, **15**, 7161 (2016).
16. J.R.Lakowicz, Principles of Fluorescence Spectroscopy, Plenum Press, New York (1999).
17. H.Homayoni, K.Jiang, X.Zou, *Photodiag. and Photodynam. Therapy*, **2**, 258 (2015).
18. J.Lee, N.Rancilio, J.Poulson, *ACS Appl. Mat. & Interfaces*, **13**, 8608 (2016).
19. Y.Yang, *Mater. Res. Innov.*, **4**, 267 (2012).
20. A.Kamkaew, F.Chen, Y.Zhan et al., *ASC Nano*, **4**, 3918 (2016).
21. UA. Patent 113942 (2017).
22. Y.Wang, B.Li, L.Zhang, *Langmuir*, **28**, 1657 (2012).
23. I.Typitsyna, P.Maksimchuk, A.Yakubovskaya et al., *Functional Materials*, **4**, 535 (2016).
24. S.Zeng, R.Tang, H.Su, *NANO: Brief Rep. and Rev.*, **4**, 1650039 (2016).
25. Y.Zhang, W.Gong, J.Yu, *The Royal Soc. Chem. Adv.*, **5**, 62527 (2015).
26. I.Tupitsyna, P.Maksimchuk, A.Yakubovskaya et al., *Functional Materials*, **1**, 16 (2017).